Molecular Therapy
Methods & Clinical Development
Original Article

Expression of Neprilysin in Skeletal Muscle by Ultrasound-Mediated Gene Transfer (Sonoporation) Reduces Amyloid Burden for AD

Yuanli Li,[1,2,6] Yadi Wang,[3,6] Jue Wang,[4] Ka Yee Chong,[2] Jingjing Xu,[2] Zhaohui Liu,[5] and Chunlei Shan[1,2]

[1]Department of Rehabilitation Medicine, Yueyang Hospital of Integrated Traditional Chinese and Western Medicine, Shanghai University of Traditional Chinese Medicine, Shanghai, 200080, China; [2]School of Rehabilitation Science, Shanghai University of Traditional Chinese Medicine, Shanghai, 201203, China; [3]Department of Surgery, Xi'an Health School, Xi'an, Shannxi 710054, China; [4]The Key Laboratory of Biomedical Information Engineering, Ministry of Education, Institute of Rehabilitation Medicine, School of Life Science and Technology, Xi'an Jiaotong University, Xi'an 710049, China; [5]Department of Rehabilitation and Physiotherapy, Tangdu Hospital, Air Force Medical University, Xi'an 710038, China

Amyloid β (Aβ) accumulation in the brain is considered to be one of the major pathological changes in the progression of Alzheimer's disease (AD). Neprilysin (NEP) is a zinc metallopeptidase that efficiently degrades Aβ. However, conventional approaches for increasing NEP levels or inducing its activation via viral-vector gene delivery have been shown to be problematic due to complications involving secondary toxicity, immune responses, and/or low gene transfer efficiency. Thus, in the present study, a physical and tractable NEP gene-delivery system via ultrasound (US) combined with microbubbles was developed for AD therapy. We introduced the plasmid, human NEP (hNEP), into skeletal muscle of 6-month-old amyloid precursor protein/presenilin-1 (APP/PS1) AD mice. Interestingly, we found a significantly reduced Aβ burden in the brain at 1 month after the delivery of overexpressed hNEP into skeletal muscle. Moreover, hNEP-treated AD mice exhibited improved performance in the Morris water maze compared to that of untreated AD mice. In addition, there were no apparent injuries in the injected muscle or in the lungs or kidneys at 1 month after the delivery of hNEP into skeletal muscle. These findings suggest that the introduction of hNEP into skeletal muscle via US represents an effective and safe therapeutic strategy for ameliorating AD-like symptoms in APP/PS1 mice, which may have the potential for clinical applications in the future.

INTRODUCTION

Alzheimer's disease (AD) has been estimated to have afflicted over 55 million individuals worldwide in the span of 2018–2019 alone, and no suitable clinical therapeutic measures are currently available. The symptoms of AD include progressive impairments in memory, communication, and thinking. Thus, there is an urgent need to explore and develop novel therapeutic strategies using drugs and gene-delivery systems/agents, either alone or in combination, for superior neuroprotection in AD to enhance the quality of life of affected individuals.[1] Accumulation of amyloid β (Aβ) in the brain is considered to represent the initial hallmark of AD pathological processes.[2,3] An imbalance between the production and clearance of Aβ results in aberrant Aβ deposits that can lead to the progression of AD.[4] Neprilysin (NEP) is an endogenous enzyme that functions as a rate-limiting step in Aβ degradation, for which its absence increases brain Aβ levels 2-fold.[5] Moreover, the level and activity of NEP *in vivo* decrease during aging.[6] In several cases of AD, NEP concentrations have been shown to be decreased in the brain, which suggests an involvement of NEP in AD pathology.[7,8] This idea is further supported by the fact that NEP knockout mice exhibit AD-like brain pathologies and behavioral dysfunctions.[7] Thus, NEP may play a major role in the clearance of Aβ and thus, may be closely related with the occurrence of AD.[9–11] Taken together, the enhancement of NEP levels and/or activities may represent a potential therapeutic strategy for ameliorating AD pathology.[12,13]

In several reports, increased NEP concentrations *in vivo* have been shown to reduce Aβ accumulation.[14,15] However, previous approaches have used viral vectors for increasing NEP, which may induce complications, such as toxicity, immunogenicity, restricted target-cell specificity, and high costs, thus limiting their widespread use in clinical applications.[16] For example, the death of a patient in an adenoviral-mediated gene therapy trial in 1999 was associated with a massive stimulation of the patient's innate immune system, causing disseminated intravascular coagulation and multiple organ failure.[17] Thus, the increase of NEP levels in the central nervous system of AD patients presents technical challenges and safety considerations that need to be addressed prior to this approach being tested in AD clinical trials. Ultrasound (US)-mediated gene transfer

Received 27 September 2019; accepted 24 December 2019;
https://doi.org/10.1016/j.omtm.2019.12.012.

[6]These authors contributed equally to this work.

Correspondence: Zhaohui Liu, Department of Rehabilitation and Physiotherapy, Tangdu Hospital, Air Force Medical University, Xi'an 710038, China.
E-mail: liliaokf@fmmu.edu.cn
Correspondence: Chunlei Shan, School of Rehabilitation Science, Shanghai University of Traditional Chinese Medicine, Shanghai 201203, China.
E-mail: shanclhappy@163.com

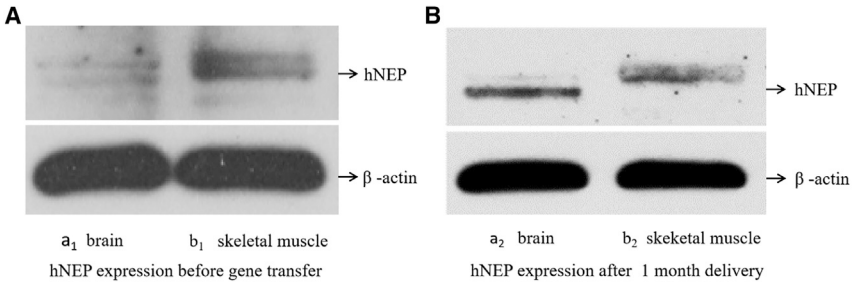

Figure 1. Expression of hNEP in Skeletal Muscle and Brains by Western Blotting

(A, a_1) hNEP expression in the brains of AD mice before hNEP gene transfer. (A, b_1) hNEP expression in skeletal muscle of AD mice before hNEP gene transfer. (B, a_2) hNEP expression in the brain of AD mice at 1 month after hNEP gene transfer by US combined with microbubble. (B, b_2) hNEP expression in skeletal muscle of AD mice at 1 month after hNEP gene transfer by US combined with microbubble. The prominent protein bands correspond to overexpression of hNEP in injected skeletal muscle and in brain tissue of the treated AD group.

(i.e., sonoporation) is one of the most promising nonviral, physical-delivery methods and involves an ultrasonic field to permeabilize cellular membranes and facilitate exogenous polynucleotide transit across the cytoplasmic membrane.[18,19] This technique is easily implemented and holds great promise for clinical gene therapy due to its low toxicity and low immunogenicity in a wide range of target tissues *in vivo*.[20,21] However, it remains unknown whether or not US-mediated NEP gene delivery effectively reduces Aβ deposits in animal models of AD.

In the present investigation, we explored the use of a novel NEP gene-delivery system via US combined with microbubbles to deliver exogenous NEP in an AD mouse model and determine its therapeutic effects. Our results demonstrate that US-mediated gene transfer of human NEP (hNEP) into skeletal muscle of amyloid precursor protein/presenilin-1 (APP/PS1) mice reduced the Aβ burden and ameliorated AD-like cognitive deficits. These findings may provide a basis for the use of the novel NEP gene-delivery system *in vivo* for ameliorating AD-like symptoms in murine models of AD, which may have the potential for clinical applications in the future.

RESULTS

hNEP Expression in Skeletal Muscle and Brain Tissue Determined by Western Blotting

As shown in Figure 1, hNEP expression in local skeletal muscle and brain tissue was detected by western blotting. As shown in Figure 1B (b_2), a band corresponding to hNEP expression was clearly observed in tissue from hNEP-treated AD mice analyzed at 1 month after hNEP gene transfer by US combined with microbubbles. A very weak band or nearly invisible band was observed before 1 month without any treatment, as shown in Figure 1A (b_1). Under normal conditions, NEP levels and activities decrease with aging; our present results provide proof of principle that US can successfully introduce exogenous hNEP plasmids into the skeletal muscle of mice. Subsequently, we tested whether hNEP gene delivery in skeletal muscle could produce hNEP overexpression in brain tissue. As shown in Figure 1B (a_2), a clearly visible band in AD mice brain tissue was seen, whereas a very weak or absent signal was observed before treatment, as shown in Figure 1A (a_1). These results demonstrate that hNEP overexpression in skeletal muscle could reach brain tissue for increasing hNEP levels in the brain.

hNEP Levels in Brain Tissue Determined by ELISA

At 1 month after NEP treatments, brain samples were collected and centrifuged, after which, they were analyzed by an enzyme-linked immunosorbent assay (ELISA) kit to detect levels of hNEP protein. As shown in Figure 2, large amounts of hNEP protein were detected in the brains of AD mice treated with hNEP gene delivery by US (sonoporation). The peak level of hNEP protein was found to be 5,800 pg/mL. In contrast, very low levels of hNEP were observed in the AD group before hNEP treatments, and the control AD mice exhibited a peak level of hNEP that was 2,300 pg/mL. The difference in hNEP levels between the hNEP-treated and untreated AD groups was statistically significant ($^*p < 0.05$). These results further confirm that US (sonoporation)-mediated delivery of hNEP into skeletal muscle resulted in increased hNEP levels in the brain of AD mice.

Aβ Deposits in the Brain Determined by Immunohistochemical Staining

We measured Aβ deposits in the brain for further assessment of the effect of hNEP in reducing Aβ burden in the brains of AD mice. Immunohistochemical staining for Aβ deposits is shown in Figure 3. Aβ was not observed in the normal control group of C57BL mice (Figures 3A and 3B). Aβ levels in the brains of AD groups, including control AD mice and experimental AD mice prior to any treatments, were the same across groups in the cortex and hippocampus (Figures 3C and 3E). However, AD mice treated with hNEP by US exhibited a >50% reduction in Aβ levels in the brain at 1 month following hNEP gene delivery (Figure 3F) compared to prior to gene delivery (Figure 3E) and untreated mice (Figure 3D). The results are consistent with the significantly increased total hNEP levels in the brains of AD mice that received hNEP gene delivery into skeletal muscle by US. These findings suggest that enhanced hNEP levels in the brain lowered Aβ deposition in AD mice.

Aβ Levels in Brain Tissue Determined by ELISA

We further quantified Aβ levels in brain tissue following hNEP gene transfer by US. At 1 month after hNEP treatments, brains were removed and centrifuged, after which, they were evaluated by ELISA. As shown in Figure 4, Aβ levels were decreased significantly in the brains of AD mice treated with hNEP gene delivery by US (sonoporation). The peak level of Aβ in the brain was 1,800 pg/mL at 1 month after hNEP delivery. However, AD mice that did not receive hNEP

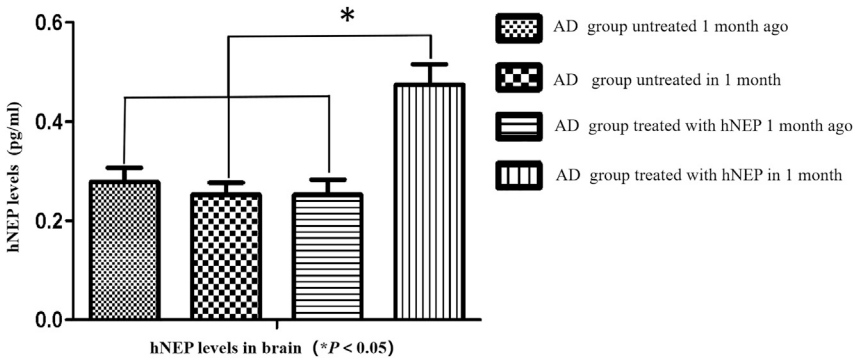

Figure 2. hNEP Levels in Brain by ELISA
The AD group that received hNEP delivery by US combined with microbubble exhibited the highest hNEP levels. These data demonstrate that hNEP levels were significantly increased in the brain following hNEP gene transfer in skeletal muscle by US.

exhibited higher levels of Aβ, at 3,500 pg/mL. Additionally, the Aβ levels after hNEP transfer by US were significantly lower than those before hNEP transfer (*p < 0.05). In contrast, there was no significant difference in the Aβ levels of the AD control group between these two time points. These data suggest that hNEP transfer into skeletal muscle via US combined with microbubbles reduced the Aβ burden in the brains of AD mice.

Performance in the Morris Water Maze

At 1 month after hNEP delivery, all mice were tested for spatial learning and memory in the Morris water maze (MWM), which is widely used for assessing cognition in mice. The latency to find and reach the hidden platform is shown in Figure 5A. The group of AD mice treated with hNEP at 1 month after US showed a significantly decreased latency to find and reach the hidden platform (24.36 ± 14.644 s) compared to that of AD mice not yet treated with hNEP (42.1 ± 14.582 s). However, AD mice that did not receive any hNEP delivery exhibited similarly long latencies to find and reach the hidden platform initially and at 1 month later (41.62 ± 18.893 s and 52.02 ± 10.573 s, respectively). Interesting, the latency to find/reach the hidden platform in AD mice without hNEP delivery was longer at testing 1 month later. This result may have been due to further increased Aβ levels exacerbating cognitive performance over time. In contrast, normal C57BL mice exhibited normal latency to find and reach the hidden platform initially and at 1 month later (24.42 ± 16.752 s and 28.98 ± 14.692 s, respectively). Moreover, the latency to find and reach the hidden platform in AD mice at 1 month after hNEP transfer by US was nearly the same as that of normal C57BL mice. Taken together, these findings suggest that hNEP gene therapy can improve AD symptoms associated with the spatial learning and memory in APP/PS1 mice.

Additionally, we found that AD mice treated with hNEP delivery by US traveled a significantly decreased distance to find and reach the hidden platform (786.38 ± 646.231 cm) compared to that prior to hNEP delivery (1,213.21 ± 568.574 cm; Figure 5B). However, the control group of AD mice without hNEP delivery exhibited similarly long distances to find/reach the hidden platform initially and at 1 month later (1,130.49 ± 513.587 cm and 1,344.4 ± 513.587 cm, respectively). In contrast, C57BL mice exhibited normal distances to find/reach the hidden platform initially and at 1 month later (861.49 ± 427.105 cm and 910.85 ± 440.132 cm, respectively). Moreover, the distance to find/reach the hidden platform in AD mice at 1 month after hNEP transfer by US became shorter obviously. These findings suggest that hNEP gene therapy via US (sonoporation) ameliorated cognitive deficits in APP/PS1 mice.

Tissue Damage Determined by Hematoxylin and Eosin (H&E) Staining

In addition, we assessed tissue damages in the injected local skeletal muscle, as well as in the lungs and kidneys, for assessing the safety of US-mediated hNEP delivery into skeletal muscle. H&E staining was assessed in slices of local skeletal muscle, lungs, and kidney tissues. As shown in Figure 6, there was no visible cellular or tissue damage observed before or after hNEP gene therapy in AD mice by US (sonoporation). These findings suggest that this approach may be safe for AD clinical applications.

DISCUSSION

AD is the most common cause of dementia and afflicts more individuals worldwide than any other neurodegenerative disease.[1] Aβ plaques and tau neurofibrillary tangles represent the primary hallmarks of AD. Aβ plaques are aberrant extracellular deposits that are considered to represent the initial pathology that ultimately leads to AD progression.[22] Many studies have focused on reducing and/or clearing Aβ depositions for AD therapy. For almost two decades, researchers in both academia and the pharmaceutical industry have been searching for a "disease-modifying" drug that arrests or reverses the severe symptoms of AD. However, the failure of these attempts is not merely due to starting drug therapy too late in the disease process (as many believe) but rather, because current drugs being clinically tested have difficulty in crossing the blood-brain barrier.[23] Recently, gene therapy has received increased attention for ameliorating AD.[24] Among these gene therapies, NEP, the major endogenous Aβ-degrading enzyme, has been investigated both *in vivo* and *in vitro*. Interestingly, NEP levels and activities *in vivo* decrease during aging. Several studies have revealed low quantities of NEP in brain regions that are vulnerable to Aβ accumulation, such as the hippocampus and associated cortices.[25] Thus, the increase of NEP levels and activities may represent a potential therapeutic strategy for ameliorating AD. Overexpression of NEP in the brains of AD animals via virus gene transfer has been shown to reduce the Aβ load and improve memory performance.[26] In consideration of future clinical applications, a NEP gene-delivery system needs to be both efficacious and safe. The rich blood supply and stable postmitotic nature of skeletal

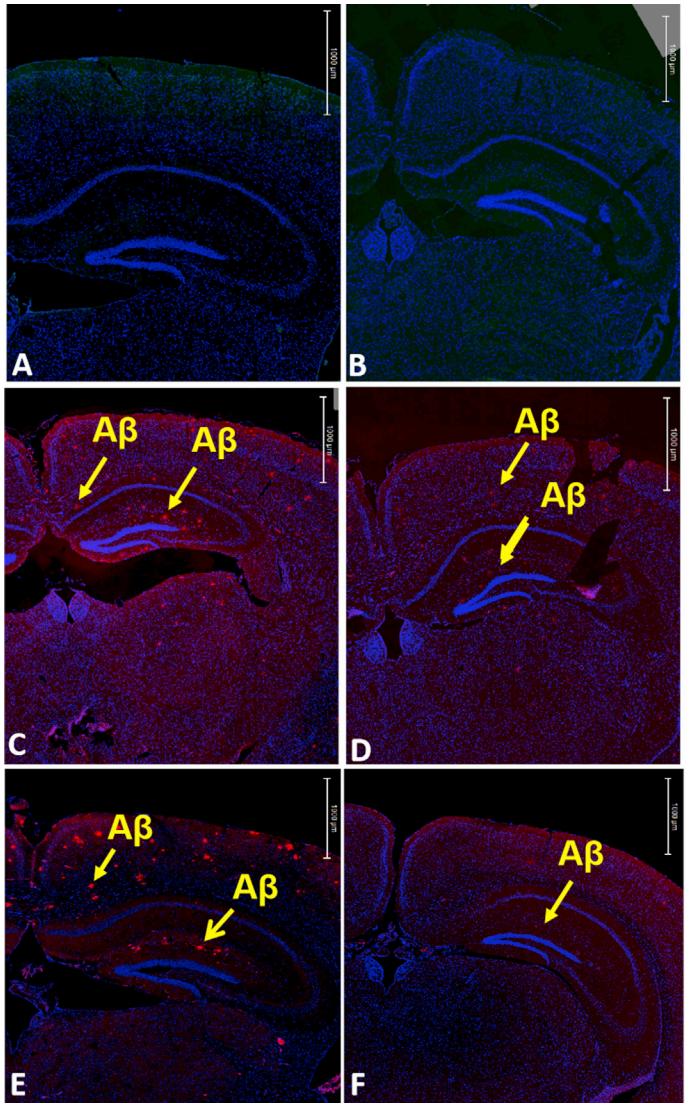

A C57/BL mice untreated 1 month ago
B C57/BL mice untreated in 1 month
C AD group untreated 1 month ago
D AD group untreated in 1 month
E AD treated group with hNEP 1 month ago
F AD treated group with hNEP in 1 month

Figure 3. Aβ Deposits in the Brain by Immunohistochemistry

Mouse brains were removed and subjected to immunohistochemistry, as described in Materials and Methods. (A and B) The brain slices of normal C57BL mice initially (A) and at 1 month later (B). (C and D) The brain slices of the untreated AD control group initially (C) and at 1 month later (D). Aβ deposits are marked by yellow arrows. (E) The brain slices of the AD experimental group at 1 month prior to hNEP delivery. More Aβ deposits were found (yellow arrows). (F) The brain slices of the AD experimental group at 1 month after hNEP delivery by US. Aβ deposits were significantly decreased in the cortex and hippocampus (scale bars, 1,000 μm).

muscle make it a promising target for genetic manipulations by both integrating and nonintegrating viral and nonviral vectors.[27] Intramuscular injection is an attractive route for the administration of nonviral gene carriers. The highly vascularized and stable nature of the skeletal muscle opens up opportunities for introducing gene-transfer agents into the systemic circulation for the treatment of human diseases distant from the site of muscle treatment.[28] For example, Liu et al.[29] reported that expression of NEP in skeletal muscle using an adeno-associated virus (AAV) reduced Aβ in a transgenic mouse model of AD. However, this previous study only measured NEP expression in injected local skeletal muscle but not in brain tissue. In our previous research to determine whether hNEP protein can pass the blood-brain barrier after gene delivery by US, we introduced the hNEP plasmid into skeletal muscle and found that hNEP protein was significantly increased in brain tissue of healthy mice; this finding demonstrates that hNEP can pass the blood-brain barrier and enter brain tissue. Additionally, this finding also provided a possibility for NEP plasmid injected into peripheral skeletal muscle to be transferred to the brain for AD therapy.[30] Importantly, viral vectors for NEP gene delivery *in vivo* or *in vitro* in AD models may be associated with complications that would prevent the use of such a therapeutic strategy in humans. Thus, an efficient and safe NEP delivery system *in vivo* needs to be established for AD gene therapy in the future.

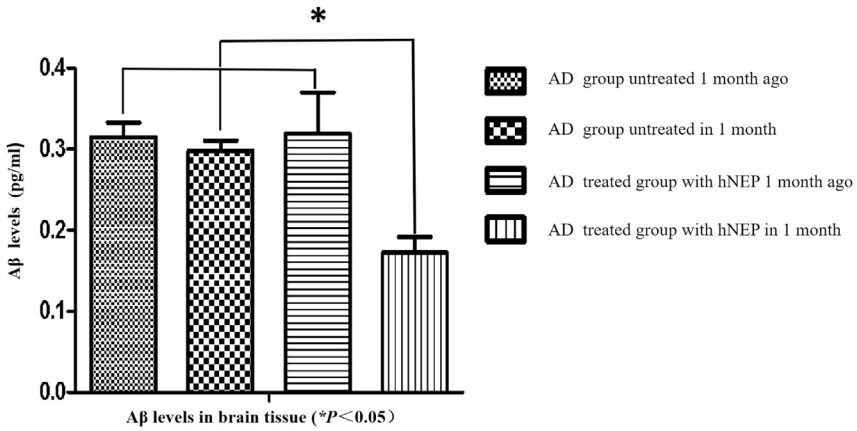

Figure 4. Aβ Levels in the Brain by ELISA
The AD group that received hNEP delivery by US exhibited the lowest Aβ levels at 1 month after hNEP delivery. These data demonstrate that Aβ levels in the brain were significantly decreased at 1 month after hNEP delivery into skeletal muscle by US.

US-mediated gene transfer has been demonstrated to represent a promising approach for stimulating uptake of therapeutic agents both *in vitro* and *in vivo*. US waves do not produce any significant adverse effects when focused on different anatomic locations in the human body. US-mediated delivery of naked plasmid DNA into muscle has been demonstrated to yield promising results.[31] However, the effect of US-mediated NEP gene delivery in AD mice has not previously been determined. In the present study, we investigated the effect of hNEP overexpression via delivery into skeletal muscle by US combined with microbubbles. We have previously shown that the US device can achieve gene transfer simultaneously with US irradiation, which can maximize the transfection rate of genes compared to that of conventional US devices. The data in our present study showed that overexpression of hNEP into local skeletal muscle by US was noticeable at 1 month after delivery (Figure 1), and significantly higher levels of brain hNEP were found in APP/PS1 mice receiving hNEP delivery compared to untreated AD mice (Figures 1 and 2). These findings suggest that hNEP delivered into skeletal muscle was able to reach the systemic circulation and cross the blood-brain barrier.

Subsequently, we found that hNEP delivery into skeletal muscle resulted in reduced Aβ levels in the brains of APP/PS1 compared to those that did not receive any treatments (Figure 3). NEP has a high affinity for Aβ *in vivo* compared to that for other small neuropeptides,[4] suggesting that upregulation of NEP may reduce Aβ and ameliorate AD-like symptoms in AD mice. Indeed, previous reports have indicated that decreasing the accumulation of Aβ can improve memory in AD mice. Here, we assessed all mice in the MWM. Interestingly, we found that US-mediated hNEP delivery into skeletal muscle of AD mice reduced latency and distances to find/reach the hidden platform compared to these parameters in untreated AD mice (Figure 5). These findings suggest that spatial memory deficits in AD mice were ameliorated after treatment with hNEP.

In addition, we investigated tissue damage in local skeletal muscle, lungs, and kidneys following US-mediated hNEP delivery into skeletal muscle. Our results showed that there were no significant injuries in any analyzed tissues. Thus, we proposed that our novel, nonviral, US-mediated gene-delivery system is safe *in vivo*.

In conclusion, our present study is the first to report a novel, nonviral gene-delivery system using US combined with microbubbles for plasmid hNEP delivery *in vivo*. However, in our present study, our analyzed APP/PS1 mice exhibited some behavioral and health issues that included the following: the main symptom was epileptic seizures during the MWM; in additional, some APP/PS1 mice died as seriously skin diseases over time. These issues may have been due to the defect of animal tolerance of APP/PS1 AD mice or very quick progression of AD pathology in the late stage of the disease, since we have previously shown that US-mediated hNEP gene transfer *in vivo* is safe in healthy mice and does not induce any complications.[30] Taken together, our nonviral hNEP delivery system via US combined with microbubbles may represent a potential approach for AD therapy. However, the half-life of NEP *in vivo* needs to be measured periodically over time in future studies.

MATERIALS AND METHODS

Materials

The hNEP plasmid that we used (PCSC-SP-PW-hNEP; 11,090 bp), as shown in Figure 7, consisting of the hNEP gene under the control of the cytomegalovirus promoter, was provided by Dr. Louis B. Hersh and Dr. Yinxing Liu (Department of Molecular and Cellular Biochemistry, University of Kentucky, Lexington, KY, USA). Microbubble reagents (USphere) were provided by United Well Technologies (Shanghai, China). Purified monoclonal antibodies (mAbs) against hNEP (anti-human CD10 mAb clone MEM-78) were obtained from BioLegend (San Diego, CA, USA). An antibody against mouse b-actin was purchased from Sigma (St. Louis, MO, USA). An hNEP/Aβ42 ELISA kit was obtained from R&D Systems (Minneapolis, MN, USA). A bicinchoninic acid (BCA) protein assay kit was purchased from Beyotime (Shanghai, China). The N terminus of Aβ42 (Ab26-2.13) was obtained from Maria Kounnas (Torrey Pines Pharmaceutical, La Jolla, CA). Horse anti-mouse conjugated to peroxidase was purchased from Vector Laboratories (Burlingame, CA, USA). The MWM was provided by Shanghai Yi Shu Technology.

Experimental Animals

6-Month-old APP/PS1 male mice (≈25 g) were obtained from the Institute of Animal Research at the Chinese Academy of Sciences (Beijing, China). This AD mouse model was derived from transgenic of C57BL mice. 6-month-old C57BL male mice (≈25 g) were

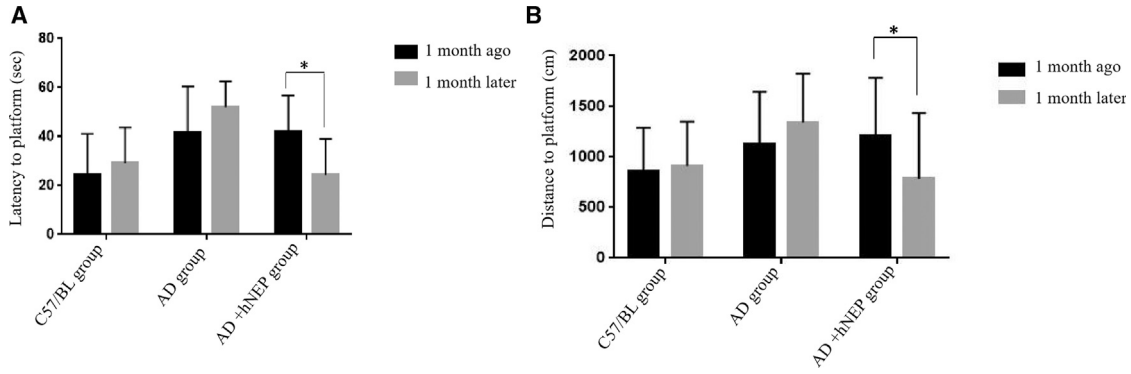

Figure 5. Latency and Distance to Find and Reach the Hidden Platform in the MWM

(A) The latency to find and reach the hidden platform of AD mice at 1 month after hNEP gene therapy by US was significantly decreased comparing that before hNEP treatment (*p = 0.0050). (B) The swimming distance to find and reach the hidden platform in AD mice with hNEP gene therapy by US was decreased significantly compared to that before treatment (*p = 0.0326).

obtained from the Experimental Animal Centre, Air Force Medical University (Xi'an, China). All animal experimental procedures were approved by the Animal Ethics Committee at Air Force Medical University and were conducted via protocols approved by the Institutional Animal Care and Use Committee.

US Apparatus

A syringe-focused US device was used according to a procedure that has been described previously.[30] Specifically, hNEP plasmids were prepared in microbubble suspensions that were then injected through the syringe simultaneously via US irradiation (1.7 MHz, 1.0 W/cm^2, and a 1-min exposure time). After completion of the experiment, the whole US transducer and syringe device were removed together. A US signal-generator device was provided by Bo You Ultrasound Technology (Xi'an, China).

Preparation of Microbubble Suspensions Containing hNEP Plasmids

We first made hNEP plasmid amplification, then we used a small extract and purification kit for hNEP plasmid extraction, and the final concentration made was 1 μg/μL. USphere microbubbles Trans+ was taken out from refrigeration and left in room temperature at about 20°C ~30°C for 30 min. Then, USphere microbubbles Trans+ activation required 40 s of shaking; a mixing ratio of 0.2~0.4 mg of DNA per bottle of Trans+ (800 μL) was recommended. We extracted microbubbles Trans+ 80 μL (0.1 mL), according to the instructions, and added 0.04 mg hNEP plasmids and sterile saline, and USphere microbubbles Trans+ hNEP 1 mL suspensions solution was mixed well. We injected 0.5 mL suspensions (containing 20 μg hNEP plasmid) into skeletal muscle of experimental mice each time.

US-Mediated Gene Transfer of Plasmid hNEP into Skeletal Muscle

Animals were divided into two experimental groups and one control group (n = 20 in each group). One experimental group was anesthetized via intraperitoneal injection of amobarbital (concentration of 0.5%, 0.01 mL/g). The right-hindlimb muscles (right [R]) of each mouse were surgically exposed, and the syringe was inserted into the gastrocnemius. Then, 20 μg of plasmid hNEP was simultaneously injected into the gastrocnemius during US irradiation (1.7 MHz, 1 W/cm^2, 1 min exposure time). This dose was determined to represent the optimal therapeutic dose in our previous studies.[30] Another experimental group of AD mice, as well as healthy C57BL mice, was not provided any treatments (no hNEP plasmid injections or US exposure). Finally, hNEP plasmid concentrations (typically 0.6 mg/mL) and purities (optical density: 260/280 nm ratios of 1.7–1.9) were evaluated by spectrophotometry.

Western Blotting of hNEP Protein

Animals were sacrificed at 1 month after hNEP gene delivery. Hindlimb muscles and brain tissues were removed and homogenized in 1 mL of cell lysis buffer (20 mM Tris-HCl, pH 7.5, 150 mM NaCl, 1% Triton X-100, sodium pyrophosphate, b-glycerophosphate, ethylenediaminetetraacetic acid [EDTA], Na_3VO_4, leupeptin, phenylmethanesulfonyl fluoride) using an Ultra-Turrax T 25 basic homogenizer (IKA, Wilmington, NC, USA). Homogenates were centrifuged at 13,000 *g* for 40 min, and supernatants were collected. Protein concentrations were determined using a BCA protein assay kit (Beyotime, Shanghai, China). Muscle and brain homogenates (10 mL) were subjected to sodium dodecyl sulfate-polyacrylamide gel electrophoresis and western blotting. Blots were incubated for 1 h at room temperature with a mouse anti-hNEP monoclonal antibody (dilution, 1:500). Mouse anti-b-actin (dilution, 1:10,000) was used as an internal control. Blots were developed with horseradish peroxidase-coupled goat anti-mouse immunoglobulin G and conventional peroxidase detection procedures.

Measurement of hNEP and Aβ Levels in Brains by ELISA

Whole-brain tissue was collected at 1 month after gene delivery in tubes containing EDTA. Tissue homogenates were centrifuged at 1,500 *g* for 10 min. Then, the supernatant was used for measurement of hNEP and Aβ levels using corresponding ELISA kits.

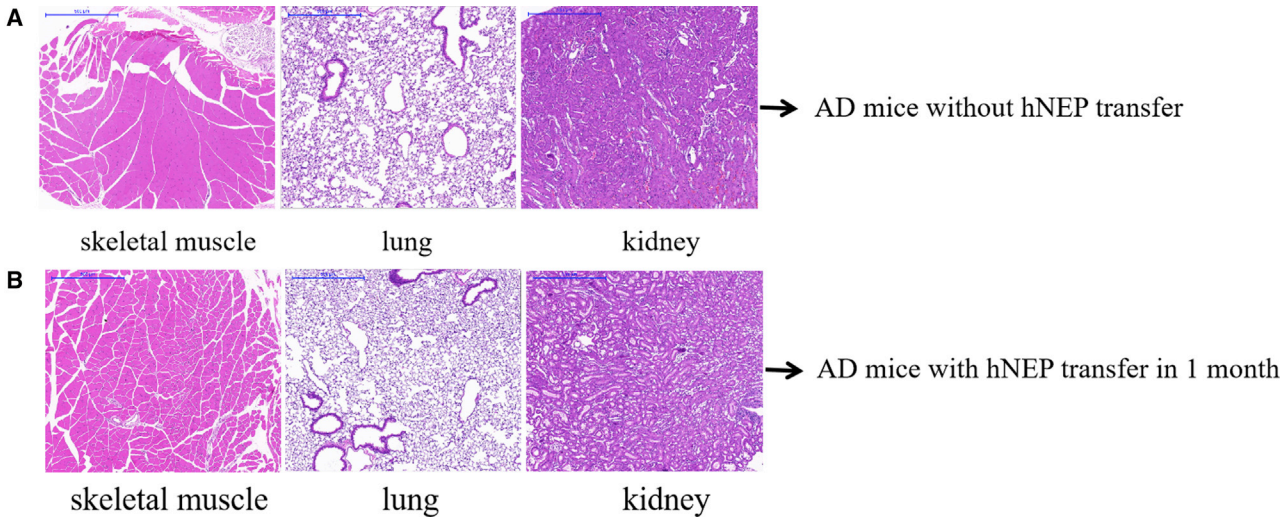

Figure 6. Tissue Damage by H&E Staining

Tissue damage was assessed in injected local skeletal muscle, as well as in lung and kidney tissues. There were no signs of visible cellular or tissue damage in the 4-μm slices of skeletal muscle, lung, and kidney tissues (scale bars, 30 μm).

Measurement of Aβ Deposits in Brains by Immunohistochemistry

Cryostat-sectioned coronal sections (16 μm) from frozen brains were fixed in 3% paraformaldehyde in PBS. Following incubation with 3% H_2O_2 to quench endogenous peroxidase activity, the sections were blocked with PBS containing 0.1% Triton X-100, 0.1% bovine serum albumin, and 2% normal horse serum for 1 h at room temperature, after which, sections were incubated overnight at 4°C with a monoclonal antibody against the N terminus of Aβ42. Sections were washed three times in PBS and were incubated with the appropriate secondary antibody—horse anti-mouse conjugated to peroxidase (1:2,500) or horse anti-rabbit conjugated to peroxidase (1:2,500; Vector Laboratories)—for 1 h at room temperature. Sections were developed with 3,3′-diaminobenzidine (DAB; Vector Laboratories). A fluorescent microscope was used for imaging.

Behavioral Testing in the MWM

The MWM is one of the most commonly used paradigms for assessing hippocampal-dependent spatial learning and memory in mouse models of AD.[32] In the MWM, a circular water tank, made from aluminum (diameter, 100 cm; height, 40 cm), was filled to a depth of 25 cm with water (23°C) and rendered opaque by the addition of a small amount of nontoxic white powder. Four positions around the edge of the tank were arbitrarily designated north (N), south (S), east (E), and west (W) to provide four alternative start positions and to define the division of the tank into four quadrants: NE, SE, SW, and NW. A square white Perspex escape platform (10 × 10 × 2 cm) was submerged 1.0 cm below the water surface and placed at the midpoint of the NE quadrant. The platform was invisible to the mice. Four visible cues to assist the mice for spatial analysis were placed outside the wall of the pool. A video camera, connected to a SMART video tracking system (San Diego Instruments, San Diego, CA, USA), was fixed 1.6 m above the center of the swim tank, and all swimming trials were recorded for further analysis. At 1 month after injections, each APP/PS1 mouse overexpressing hNEP was trained for 4 consecutive days to find and reach the hidden platform from the four different starting points. Starting points were randomized every day during the 4 days of trials. Each mouse was placed gently in the pool facing the tank wall. Every mouse was allowed to swim and reach the platform within 60 s (spatial learning). If the mouse reached the platform, it was allowed to stay on the platform for another 30 s. If the mouse failed to reach the platform, it was gently placed on the platform for 30 s. Before the next trial, each mouse was allowed to rest for 10 min. On the day after the last training session, the platform was removed, and each mouse was allowed to search for the platform within 60 s (memory retention). To compare the spatial learning and memory retention between untreated mice and those overexpressing hNEP, the escape latencies and distances taken by the mice to reach the platform were measured at 1 month following hNEP treatments.

Measurement of Cellular and Tissue Damage by H&E Staining

Cellular and tissue damage was evaluated by H&E staining. Briefly, local-injected skeletal muscle, as well as lungs and kidneys, was removed and immediately fixed with 4% paraformaldehyde and embedded in paraffin. 4 μ Slices were prepared for H&E staining. A computer-assisted light microscope (IX51; Olympus) was used to scan the sections.

Statistical Analysis

Data are presented as the mean ± SEM and were analyzed by one-way analysis of variance (ANOVA) using SPSS, version 23.0 (SPSS,

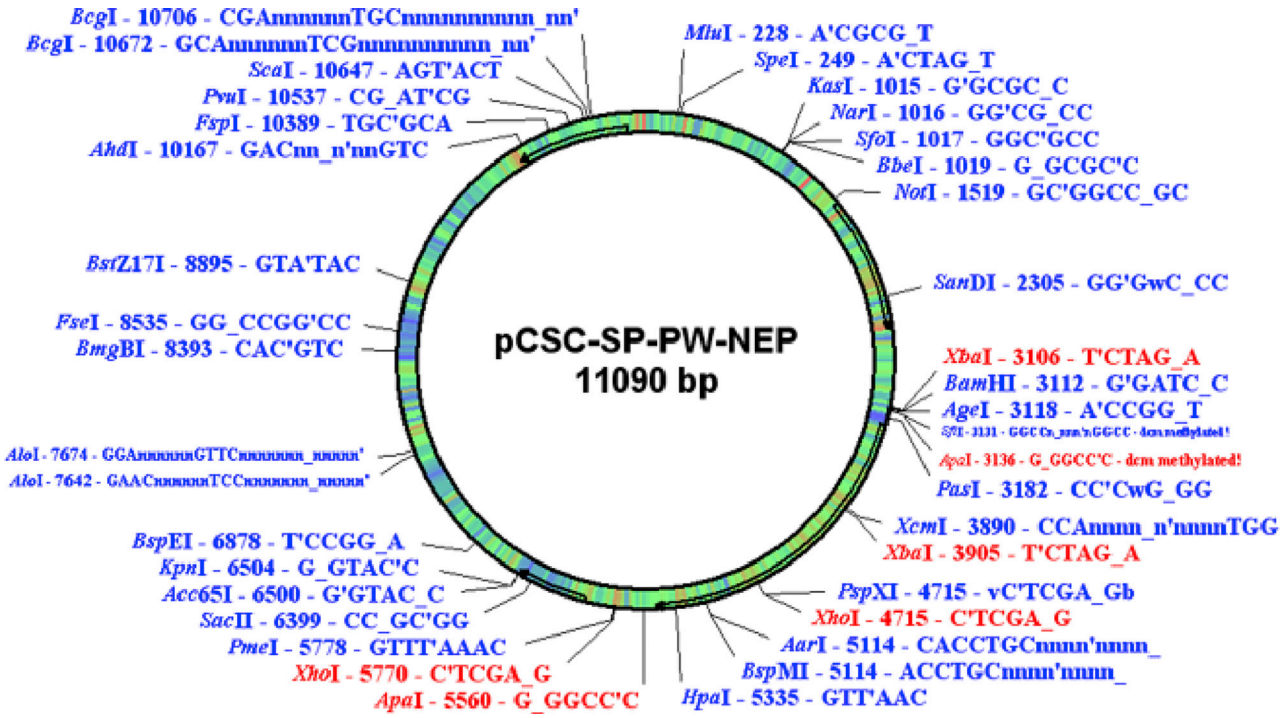

Figure 7. hNEP Gene Map

The hNEP gene sequence was inserted into two sites between BamHI and XhoI (BamHI–XhoI).

Chicago, IL, USA). For all comparisons, a difference with a p value less than 0.05 was considered statistically significant.

AUTHOR CONTRIBUTIONS

Y.L. conceived and designed the study. Y.W performed the experiments and analyzed the data. J.W. designed and provided the US device and its parameters. K.Y.C. and J.X. wrote the English revision of the manuscript. Z.L. provided more guidance to Wangdi Wang for carrying out experimental protocols. C.S. provided more guidance to Y.L. for writing the manuscript, figure production, and experimental design. All authors reviewed the manuscript and contributed to its writing.

CONFLICTS OF INTEREST

The authors declare no competing interests.

ACKNOWLEDGMENTS

The authors thank Dr. Louis B. Hersh and Dr. Yinxing (Department of Molecular and Cellular Biochemistry, University of Kentucky) for providing hNEP plasmids. This work was supported by theNational Natural Science Foundation (grant nos. 81301076 and 81874035); China Postdoctoral Science Foundation; Shanghai Health Commission's Rehabilitation Diagnosis and Treatment Promotion Project of Integrated Traditional Chinese and Western Medicine (grant no. ZY (2018-2020)-FWTX-8002); and Shanghai Health Commission Accelerating the Development of Traditional Chinese Medicine Three-Year Action Plan Project (grant no. ZY (2018-2020)-CCCX-2001-06/2004-05).

REFERENCES

1. Wortmann, M. (2012). Dementia: a global health priority - highlights from an ADI and World Health Organization report. Alzheimers Res. Ther. *4*, 40.

2. Capetillo-Zarate, E., Gracia, L., Tampellini, D., and Gouras, G.K. (2012). Intraneuronal Aβ accumulation, amyloid plaques, and synapse pathology in Alzheimer's disease. Neurodegener. Dis. *10*, 56–59.

3. Goldsworthy, M.R., and Vallence, A.M. (2013). The role of β-amyloid in alzheimer's disease-related neurodegeneration. J. Neurosci. *33*, 12910–12911.

4. Mazur-Kolecka, B., and Frackowiak, J. (2006). Neprilysin protects human neuronal progenitor cells against impaired development caused by amyloid-beta peptide. Brain Res. *1124*, 10–18.

5. Nilsson, P., Loganathan, K., Sekiguchi, M., Winblad, B., Iwata, N., Saido, T.C., and Tjernberg, L.O. (2015). Loss of neprilysin alters protein expression in the brain of Alzheimer's disease model mice. Proteomics *15*, 3349–3355.

6. Hüttenrauch, M., Baches, S., Gerth, J., Bayer, T.A., Weggen, S., and Wirths, O. (2015). Neprilysin deficiency alters the neuropathological and behavioral phenotype in the 5XFAD mouse model of Alzheimer's disease. J. Alzheimers Dis. *44*, 1291–1302.

7. Wang, D.S., Lipton, R.B., Katz, M.J., Davies, P., Buschke, H., Kuslansky, G., Verghese, J., Younkin, S.G., Eckman, C., and Dickson, D.W. (2005). Decreased neprilysin immunoreactivity in Alzheimer disease, but not in pathological aging. J. Neuropathol. Exp. Neurol. *64*, 378–385.

8. Sharma, H.S., Muresanu, D.F., Castellani, R.J., Nozari, A., Lafuente, J.V., Tian, Z.R., Ozkizilcik, A., Manzhulo, I., Mössler, H., and Sharma, A. (2019). Nanowired delivery of cerebrolysin with neprilysin and p-Tau antibodies induces superior neuroprotection in Alzheimer's disease. Prog. Brain Res. *245*, 145–200.

9. El-Amouri, S.S., Zhu, H., Yu, J., Marr, R., Verma, I.M., and Kindy, M.S. (2008). Neprilysin: an enzyme candidate to slow the progression of Alzheimer's disease. Am. J. Pathol. *172*, 1342–1354.

10. Hersh, L.B., and Rodgers, D.W. (2008). Neprilysin and amyloid beta peptide degradation. Curr. Alzheimer Res. *5*, 225–231.

11. Wang, H.Z., Bi, R., Zhang, D.F., Li, G.D., Ma, X.H., Fang, Y., Li, T., Zhang, C., and Yao, Y.G. (2016). Neprilysin Confers Genetic Susceptibility to Alzheimer's Disease in Han Chinese. Mol. Neurobiol. *53*, 4883–4892.

12. Nalivaeva, N.N., Fisk, L.R., Belyaev, N.D., and Turner, A.J. (2008). Amyloid-degrading enzymes as therapeutic targets in Alzheimer's disease. Curr. Alzheimer Res. *5*, 212–224.

13. Klein, C., Roussel, G., Brun, S., Rusu, C., Patte-Mensah, C., Maitre, M., and Mensah-Nyagan, A.G. (2018). 5-HIAA induces neprilysin to ameliorate pathophysiology and symptoms in a mouse model for Alzheimer's disease. Acta Neuropathol. Commun. *6*, 136.

14. Guan, H., Liu, Y., Daily, A., Police, S., Kim, M.H., Oddo, S., LaFerla, F.M., Pauly, J.R., Murphy, M.P., and Hersh, L.B. (2009). Peripherally expressed neprilysin reduces brain amyloid burden: a novel approach for treating Alzheimer's disease. J. Neurosci. Res. *87*, 1462–1473.

15. Liu, Y., Studzinski, C., Beckett, T., Murphy, M.P., Klein, R.L., and Hersh, L.B. (2010). Circulating neprilysin clears brain amyloid. Mol. Cell. Neurosci. *45*, 101–107.

16. Boulaiz, H., Marchal, J.A., Prados, J., Melguizo, C., and Aránega, A. (2005). Non-viral and viral vectors for gene therapy. Cell. Mol. Biol. *51*, 3–22.

17. Raper, S.E., Chirmule, N., Lee, F.S., Wivel, N.A., Bagg, A., Gao, G.P., Wilson, J.M., and Batshaw, M.L. (2003). Fatal systemic inflammatory response syndrome in a ornithine transcarbamylase deficient patient following adenoviral gene transfer. Mol. Genet. Metab. *80*, 148–158.

18. Huang, S., Ren, Y., Wang, X., Lazar, L., Ma, S., Weng, G., and Zhao, J. (2019). Application of Ultrasound-Targeted Microbubble Destruction-Mediated Exogenous Gene Transfer in Treating Various Renal Diseases. Hum. Gene Ther. *30*, 127–138.

19. Taniyama, Y., Tachibana, K., Hiraoka, K., Aoki, M., Yamamoto, S., Matsumoto, K., Nakamura, T., Ogihara, T., Kaneda, Y., and Morishita, R. (2002). Development of safe and efficient novel nonviral gene transfer using ultrasound: enhancement of transfection efficiency of naked plasmid DNA in skeletal muscle. Gene Ther. *9*, 372–380.

20. Li, Y., Wang, J., Satterle, A., Wu, Q., Wang, J., and Liu, F. (2012). Gene transfer to skeletal muscle by site-specific delivery of electroporation and ultrasound. Biochem. Biophys. Res. Commun. *424*, 203–207.

21. Xenariou, S., Liang, H.D., Griesenbach, U., Zhu, J., Farley, R., Somerton, L., Singh, C., Jeffery, P.K., Scheule, R.K., Cheng, S.H., et al. (2010). Low-frequency ultrasound increases non-viral gene transfer to the mouse lung. Acta Biochim. Biophys. Sin. (Shanghai) *42*, 45–51.

22. Adlard, P.A., James, S.A., Bush, A.I., and Masters, C.L. (2009). beta-Amyloid as a molecular therapeutic target in Alzheimer's disease. Drugs Today (Barc) *45*, 293–304.

23. Pardridge, W.M. (2009). Alzheimer's disease drug development and the problem of the blood-brain barrier. Alzheimers Dement. *5*, 427–432.

24. Cummings, J., Lee, G., Ritter, A., and Zhong, K. (2018). Alzheimer's disease drug development pipeline: 2018. Alzheimers Dement. (N. Y.) *4*, 195–214.

25. Turner, A.J., Isaac, R.E., and Coates, D. (2001). The neprilysin (NEP) family of zinc metalloendopeptidases: genomics and function. BioEssays *23*, 261–269.

26. Li, Y., Wang, J., Zhang, S., and Liu, Z. (2015). Neprilysin gene transfer: A promising therapeutic approach for Alzheimer's disease. J. Neurosci. Res. *93*, 1325–1329.

27. Boisgerault, F., and Mingozzi, F. (2015). The Skeletal Muscle Environment and Its Role in Immunity and Tolerance to AAV Vector-Mediated Gene Transfer. Curr. Gene Ther. *15*, 381–394.

28. Ijiri, D., Saegusa, A., Matsubara, T., Kanai, Y., and Hirabayashi, M. (2012). In vivo gene transfer into skeletal muscle of neonatal chicks by electroporation. Anim. Sci. J. *83*, 504–509.

29. Liu, Y., Studzinski, C., Beckett, T., Guan, H., Hersh, M.A., Murphy, M.P., Klein, R., and Hersh, L.B. (2009). Expression of neprilysin in skeletal muscle reduces amyloid burden in a transgenic mouse model of Alzheimer disease. Mol. Ther. *17*, 1381–1386.

30. Li, Y., Wang, J., Grebogi, C., Foote, M., and Liu, F. (2012). A syringe-focused ultrasound device for simultaneous injection of DNA and gene transfer. J. Gene Med. *14*, 54–61.

31. Bastarrachea, R.A., Chen, J., Kent, J.W., Jr., Nava-Gonzalez, E.J., Rodriguez-Ayala, E., Daadi, M.M., Jorge, B., Laviada-Molina, H., Comuzzie, A.G., Chen, S., and Grayburn, P.A. (2017). Engineering brown fat into skeletal muscle using ultrasound-targeted microbubble destruction gene delivery in obese Zucker rats: Proof of concept design. IUBMB Life *69*, 745–755.

32. Gallagher, M., Burwell, R., and Burchinal, M. (1993). Severity of spatial learning impairment in aging: development of a learning index for performance in the Morris water maze. Behav. Neurosci. *107*, 618–626.